Increasing Reliability of Price Signals in Long Term Energy Management Problems

Guillaume Erbs* Clara Lage† Claudia Sagastizábal‡ Mikhail Solodov§

October 14, 2020

Abstract

Determining reliable price indicators in the long-term is fundamental for optimal management problems in the energy sector. In hydro-dominated systems, the random components of rain and snow that arrive to the reservoirs have a significant impact on the interaction of the low-cost technology of hydro-generation with more expensive ones. The sample employed to discretize uncertainty changes certain Lagrange multipliers that represent a marginal cost for the power system and, therefore, changes the price signals. The effect of sampling in yielding different price indicators can be observed even when running twice the same code on the same computer. Although such values are statistically correct, the variability on the dual output puts at stake economic analyses based on marginal prices. To address this issue, we propose a dual regularization that yields reliable indicators for a two-stage stochastic model. It is shown that the approach provides the minimal-norm multiplier of the energy management problem in the limit, when certain parameter is driven to zero. The new method is implemented in a rolling horizon mode for a real-life case, representing the Northern European energy system over a period of one year with hourly discretization. When compared to SDDP, an established method in the area, the approach yields a significant reduction in the variance of the optimal Lagrange multipliers used to compute the prices.

1 Introduction

Energy problems provide a fertile field for application of mathematical optimization, [20], [3], [25], [15], [18]. Modern energy markets involve a large number of technologies to generate electricity and finding the best policy with lower prices is a challenging problem, [24]. This work considers long term problems that Independent System Operators and agents in the business solve to obtain price signals for hydro-dominated electric systems, similar to the setting in [4], [14], [5]. Hydro-power has the particular capacity of providing a reserve of energy in the form of water in the reservoirs. Since hydro-generation is cheaper than other sources, in places like Brazil and North Europe a sound hydro-power management in the long term is absolutely essential for the proper functioning of the whole energy system.

*ENGIE, 1 pl. S. de Champlain, 92930 Paris La Défense, France. Email:guillaume.erbs@engie.com

†ENGIE, CIFRE contract with Université de Paris Sorbonne, France; joint PhD with IMPA – Instituto de Matemática Pura e Aplicada, Brazil. Email: clarinhalage@gmail.com

‡IMECC - UNICAMP, 13083-859, Campinas, SP, Brazil. Email: sagastiz@unicamp.br. Adjunct Researcher. Partly supported by CEPID CEMEAI, FAPERJ, and CNPq Grant 306089/2019-0.

§IMPA – Instituto de Matemática Pura e Aplicada, Estrada Dona Castorina 110, Jardim Botânico, Rio de Janeiro, RJ 22460-320, Brazil. Email: solodov@impa.br. Research of this author is supported in part by CNPq Grant 303913/2019-3, by FAPERJ Grant E-26/202.540/2019, and by PRONEX–Optimization.

Uncertainty in this setting plays a prominent role, as streamflow impact on the reservoir volumes, and their level can deeply affect decisions to be taken. These problems are usually solved by sampling methods such as the well-known *Stochastic Dual Dynamic Programming* (SDDP) method [17]; see also [16]. The uncertain data is a sample with a set of scenarios, to which some probability is attached. In the optimization problem, the objective function includes thermal generation costs and load-shedding penalties, and in addition to operational constraints, generation must meet the demand along the time horizon. The growth rate of the overall cost with respect to the demand, or long-term marginal cost, is averaged over the different scenarios to compute a price signal. In energy optimization terms, the price signal is related with the Lagrange multiplier associated at an optimum with the demand constraint.

Having different scenarios for the streamflow results in different generation schedules to attend the demand, and in different price signals. In the energy sector, price signals obtained with fundamental models of the power system are used to guide the business decisions. Suppose the company has two managers, say in two different locations. Each manager determines price signals using a sample of the same size, but not necessarily the *same scenarios*. The underlying belief is that, if the samples are sufficiently large, the multiplier empirical distributions obtained with both samples will be alike. Hence, the two averaged prices will be similar; in some sense, statistically the same. This is clearly desirable since then, as common sense dictates in this situation, our two managers are likely to take similar business decisions. However, this is not what can be observed, even in very simple examples. Being assimilated to a dual variable in an optimization problem that often has a polyhedral feasible set, the price signal exhibits sharp variations and can lead to a very different output. In the simple problem we use as an illustration in Sections 3.1 and 3.3, the correct mean price signal is 0, but one manager obtains a positive price while the other manager obtains the negative of the same value, only because of the difference in the respective samples.

In order to address this issue, in [12] we introduced a dual regularization approach to stabilize Lagrange multipliers in two-stage stochastic programs. This is achieved by adding to the recourse function a penalty given by a factor of certain square norm; see Section 3.2. The new recourse function enjoys sound mathematical properties and, in the limit (as the penalizing factor goes to zero), provides primal and dual solutions to the original problem. Most importantly, our approach yields the minimal norm price signal in the multiplier set. The interest of this result is clear, since it provides a mechanism of selection that is systematic, independent of the specific run. The approach, which passes through a variational analysis and non-linear computational analysis perspectives, was developed in [12] for a setting without upper bounds. Since variables like generation and reservoir volumes are naturally bounded above, in this work we extend the theory in [12] to make it applicable to energy problems.

The stochastic programming literature on stability is abundant when it comes to primal variables, ([11], [10], [13], [2]). The analysis of multipliers, or dual variables, is a different matter. The only other study that we are aware of is [25], which deals with a problem in energy optimization, as in this work, but adopts a different perspective. The approach therein is employed to solve a short-term electricity production management problem that has 10^6 variables and 10^6 constraints. For a power system with 200 plants, the model covers 48 hours that are discretized in half-hour steps, see [7]. Because of the large scale and the practical necessity of solving the problem in a couple of hours at most, certain subproblems that arise when applying Lagrangian relaxation cannot be solved to optimality. The (inexact) oracle computing the problem data returns an approximation that causes instability in the dual solution, when considering consecutive time steps (electricity prices are not meant to jump in a bang-bang from one half hour to the next one). This phenomenon occurs even when the inaccuracy is small. The article [25] proposes a regularization with respect to *total variation* of price signals that yields satisfactory results when a bundle method handles the inexactness. In the context of our work, uncertainty is in perturbations of the right-hand side of some equality constraints of the stochastic optimization problem. We are interested in controlling the instability with respect to samples, and not with respect to time. Rather than modulating the accuracy of information used to iteratively determine optimal Lagrange multipliers, our aim is to maintain low the variance of the perturbation induced by a sampling process.

The contributions of this work are twofold. On the theoretical side, we extend the convergence theorems in [12] to a more general feasible set, with box constraints, as needed for energy management problems. These results establish the link between the dual regularized problem and the original one, and, most importantly, provide a way to find the minimal norm price signal in the multipliers set. Also, we fully solve an analytical example that illustrates the aforementioned price instability and its remedy. The second line of contributions is in the modeling and computational areas. We show the effectiveness of our approach on a real-life case covering the Northern European region. Since our work deals with two-stage programs, that long term multi-stage problem is solved by putting in place a rolling-horizon solving mechanism as in [6]; see also [1]. The procedure moves week by week over a year, solving 53 two-stage stochastic programs in succession (one per week of the year). Each one week two-stage problem is regularized using our approach. The resulting output provides input for the problem of the next week, therefore yielding an implementable policy. The rolling-horizon policy is benchmarked against SDDP, by simulating the system operation over a high number of randomly generated scenarios, covering a large spectrum of foreseeable futures. In the numerical assessment, that confirm the theoretical results, we analyze the price distribution as well as the impact of regularization on the reservoirs levels, the hydro-generation, and the interconnections between zones.

This work is organized as follows. The energy management problem and its notation is introduced in Section 2. As our application is for the Northern European market, we focus on this particular energy system, even if the model can also used for other regions with important participation of hydro-power plants, including the Brazilian case. Section 3 examines the corresponding price signals, illustrating with an analytical example their instability and explaining the dual regularization proposed as stabilizing mechanism. In particular, Subsection 3.4 is devoted to asymptotic results that describe the behavior of primal and dual regularized solutions when the regularized problem approaches the original one. Finally, in Section 4 we present numerical results for the Northern European energy system, including a comparison of the performance of SDDP against our method, implemented in a rolling-horizon mode.

2 Formulation of the energy management problem

We are interested in the problem of managing in an optimal manner the generation of an energy system, over a time horizon of 12 months, with weekly discretization. Generation optimization problems in the long term can be found in the literature, with variations in the problem to be solved, such as [7], [22], [5].

2.1 System and Nomenclature

Energy systems like the Northern European considered in our numerical experience involve several balancing zones, as illustrated by the diagram in Figure 1. A zone can be a country (say Finland) or a region in a country (say Norway 1 to Norway 5). Typically, intra-zone constraints are demand satisfaction and water balance equations, while the overall balance of the system is achieved by interconnections between the zones, as represented by the diagram in Figure 1.

Figure 1: Energy system with balancing zones

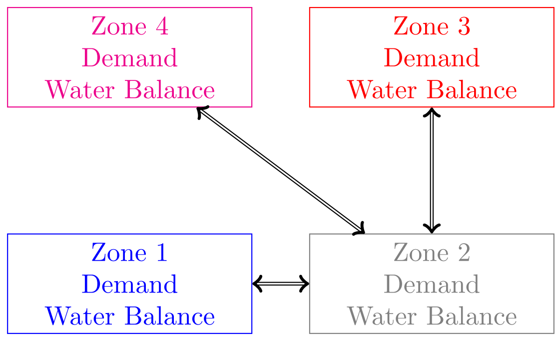

The notation for the different elements defining the optimization problem is given below.

- **Sets:**
  - Scenarios $s \in \mathbb{S}$ each one with probability p^s, representing uncertainty ξ^s on water inflows, changing the hydro power availability.
  - Time steps in the set $\{t \in \mathbb{T}\}$.
  - Balancing zones $\{z_l, l \in \mathbb{L}\}$.
  - A zone z_l has thermal power plants $\{i \in \mathbb{I}_l\}$ and hydro-plants $\{j \in \mathbb{J}_l\}$.
  - For each $l \in \mathbb{L}$, $\mathbb{F}_l$ is a set of zones connected with z_l, to import or export energy. When the zone has no connections, this set is empty.
- **Variables at time t:**
  - A hydro-plant $j \in \mathbb{J}_l$ has reservoir level v_j^t and spillage sp_j^t.
  - The generated energy of thermal and hydro-power plants gt_i^t. and gh_j^t, respectively.
  - For each $l \in \mathbb{L}$ having nonempty set $\mathbb{F}_l$, and for all $l_1 \in \mathbb{F}_l$, the energy exchanged between zones z_l and z_{l_1} is $f^t_{l \leftrightarrow l_1}$.
  - A possible deficit in generation of zone z_l is represented by an artificial power plant in the set $\mathbb{I}_l$, with very high generating cost and large capacity.
- **Parameters:**
  - For the reservoir in hydro-plant $j \in \mathbb{J}_l$, the water inflow $\mathcal{I}_j^{t,s} = \mathcal{I}_j^s(\xi^s)$, noting that for $t = 1$ this is a deterministic value: $\mathcal{I}_j^{1,s} = \mathcal{I}_j^1$, the same for all scenarios s. The reservoir initial volume is v_j^0, its maximum and minimum levels are $\underline{v}_j$ and $\bar{v}_j$, respectively.
  - For thermal power plant $i \in \mathbb{I}_l$ at time t, its maximum generation capacity $\overline{gt}_i^t$ and unit generation cost C_i^t.
  - The hydro-cost of hydro-power plant $j \in \mathbb{J}_l$ is null, and its maximum capacity $\overline{gh}_j^t$.
  - The bounds for the forward flow on interconnection between $l \in \mathbb{L}$ and $l_1 \in \mathbb{F}_l \neq \emptyset$ at time t is $\overline{f}^t_{l \leftrightarrow l_1}$. Similarly, the bound for the backward flow is $\underline{f}^t_{l \leftrightarrow l_1}$.
  - For zone z_l at time t, the deterministic demand $\mathcal{D}_l^t$.

We now explain how to deal with uncertainty, in two stages.

2.2 Two-stage stochastic programming model

For a fixed scenario s, the deterministic formulation for the problem of interest is

$$\left\{\begin{array}{llll} \min & \sum_{t\in\mathbb{T}}\sum_{l\in\mathbb{L}}\sum_{i\in\mathbb{I}_l} C_i^t gt_i^t & & \\ \text{s.t.} & \underline{v}_j^t \leqslant v_j^t \leqslant \overline{v}_j^t \text{ and } 0 \leqslant sp_j^t, & j\in\mathbb{J}_l, l\in\mathbb{L}, & t\in\mathbb{T} \\ & 0 \leqslant gh_j^t \leqslant \overline{gh}_j^t, \quad \underline{0 \leqslant gt_i^t} \leqslant \overline{gt}_i^t, & j\in\mathbb{J}_l, i\in\mathbb{I}_l, l\in\mathbb{L}, & t\in\mathbb{T} \\ & -\underline{f_{l\leftrightarrow l_1}^t} \leqslant f_{l\leftrightarrow l_1}^t \leqslant \overline{f_{l\leftrightarrow l_1}^t}, & l\in\mathbb{L}: l_1\in\mathbb{F}_l\neq\emptyset & t\in\mathbb{T} \\ & v_j^t - v_j^{t-1} + gh_j^t + sp_j^t \quad = \quad \mathcal{I}_j^{t,s}, & j\in\mathbb{J}_l, l\in\mathbb{L} & t\in\mathbb{T} \\ & \sum_{j\in\mathbb{J}_l} gh_j^t + \sum_{i\in\mathbb{I}_l} gt_i^t + \sum_{l_1\in\mathbb{F}_l\neq\emptyset} f_{l\leftrightarrow l_1}^t \quad = \quad \mathcal{D}_l^t, & l\in\mathbb{L}, & t\in\mathbb{T}. \end{array}\right. \tag{1}$$

Recall the demand equation involves no variables $f_{l\leftrightarrow l_1}^t$ for zones z_l without interconnections, as in this case $\mathbb{F}_l = \emptyset$. Note also that feasibility is ensured by the spillage and deficit (the artificial power plant generation), which act as slack variables in the equality constraints.

For legibility, the stochastic version of the linear program (1) is now cast in an abstract format, more suitable for our developments. To this aim, we adopt a two-stage approach to handle uncertainty, splitting the time steps into two sets, $\mathbb{T}_1 := \{t\in\mathbb{T} : t \leqslant t_1\}$ and $\mathbb{T}_2 := \{t\in\mathbb{T} : t > t_1\}$. Until time t_1 all data is known, with scenarios s corresponding to right-hand side uncertainty, relative to times in $\mathbb{T}_2$:

$$\left\{\begin{array}{lll} \min & \langle F_1, x_1\rangle + \sum_{s\in\mathbb{S}} p^s \langle F_2, x_2^s\rangle & \\ \text{s.t.} & 0 \leqslant x_1 \leqslant b_1 & \\ & 0 \leqslant x_2^s \leqslant b_2 & \text{for } s\in\mathbb{S} \\ & Tx_1 + Wx_2^s = h^s & \text{for } s\in\mathbb{S}. \end{array}\right. \tag{2}$$

The difference between (2) and the problems considered in [12] is in the upper bounds ($x \leqslant b$). The formulation in [12] corresponds to taking $b = +\infty$. Box constraints were not present in that work but they are necessary in our energy problem. The new setting with more constraints changes the multiplier set and for this reason requires a new convergence analysis, see Theorem 3.2.

As mentioned, the one-year horizon in our energy management problem (2) is handled in a rolling-horizon mode, considering a sequence of two-stage programs (2), each one with $\mathbb{T}_1$ representing the number of hours in the first week under consideration (and $\mathbb{T}_2$ the rest of the year); details are given in Section 4.1.1 below.

The relation between the abstract notation and the one in (1) is the following. Variables with time index $t \leqslant t_1$ define the first-stage decision vector

$$x_1 := \bigcup_{t\in\mathbb{T}_1} \left\{ \left(v_j^t, sp_j^t, gh_j^t\right)_{j\in\mathbb{J}_l}, (gt_i^t)_{i\in\mathbb{I}_l}, (f_{l\leftrightarrow l_1}^t)_{l_1\in\mathbb{F}_l\neq\emptyset}\right) : l\in\mathbb{L} \right\}, \tag{3}$$

which is of "here-and-now" type. Since we consider that uncertainty reveals at time t_1, all variables with index $t > t_1$ are of the "wait-and-see" type and, hence, denoted by x_2^s for each scenario s:

$$x_2^s := \bigcup_{t\in\mathbb{T}_2} \left\{ \left(v_j^{t,s}, sp_j^{t,s}, gh_j^{t,s}\right)_{j\in\mathbb{J}_l}, (gt_i^{t,s})_{i\in\mathbb{I}_l}, (f_{l\leftrightarrow l_1}^{t,s})_{l_1\in\mathbb{F}_l\neq\emptyset}\right) : l\in\mathbb{L} \right\}.$$

The objective in (1) is likewise split, so that we have vectors F_1 and F_2 of appropriate dimensions satisfying

$$\sum_{t\in\mathbb{T}_1}\sum_{l\in\mathbb{L}}\sum_{i\in\mathbb{I}_l} C_i^t gt_i^t = \langle F_1, x_1\rangle \quad \text{and} \quad \sum_{t\in\mathbb{T}_2}\sum_{l\in\mathbb{L}}\sum_{i\in\mathbb{I}_l} C_i^t gt_i^{t,s} = \langle F_2, x_2^s\rangle .$$

In a manner similar, the box constraints in (1), written for x_1 and x_2^s, are rewritten

$$x_1 \leqslant b_1 \quad \text{and} \quad x_2^s \leqslant b_2\,, s \in \mathbb{S}\,,$$

taking appropriate vectors b_1 and b_2. Although not present in (1), explicit upper bounds for the spillage and interconnections (variables sp_j^t and $f_{l\leftrightarrow l_1}^t$) can be obtained from the water balance and demand equality constraints.

Finally, notice that in (1) only the water balance equations couple time steps. In particular, for $t = t_1 + 1$, this gives an equality coupling components of x_2^s with components of x_1:

$$v_j^{t_1+1,s} - v_j^{t_1} + gt_j^{t_1+1,s} + sp_j^{t_1+1,s} = \mathcal{I}_j^{t_1+1,s}, j \in \mathbb{J}_l\,, l \in \mathbb{L}\,.$$

As usual in stochastic programming, this relation is expressed as

$$Tx_1 + Wx_2^s = h^s\,,$$

where the vector $h^s = h(\xi^s)$ has components given by the right-hand side terms $\mathcal{I}_j^{t,s}$ and $\mathcal{D}_{l_1}^t$. In the abstract format, the demand equation:

$$\sum_{j\in\mathbb{J}_l} gh_j^t + \sum_{i\in\mathbb{I}_l} gt_i^t + \sum_{l_1\in\mathbb{F}_l\neq\emptyset} f_{l\leftrightarrow l_1}^t = \mathcal{D}_l^t,\ l \in \mathbb{L}\ t \in \mathbb{T}\,,$$

is also incorporated in the constraint $Tx_1 + Wx_2^s = h^s$, by taking technology and recourse matrices T and W of appropriate dimensions.

3 Reliability of price signals

The price signals given by the demand constraint correspond to components of the optimal multiplier associated with the last constraints in (2), with right-hand side vector h^s, for $s \in \mathbb{S}$. As mentioned, a common practice in the energy sector is to average those signals and use the resulting mean price to guide the company business strategies.

We start with a simple example showing that for the energy management problem (2) taking different scenario sets $S_1 \neq S_2$ (with the same cardinality) can yield very different averaged prices. We then extend to the box-constrained setting to the box-constrained setting the stabilizing procedure introduced in [12], and show its convergence.

3.1 An illustrative particular case

Suppose in (2) the right-hand side vector $h_s = \xi_s$ is a particular realization of the continuous variable $\xi \in \mathbb{R}$, with cumulative distribution function denoted by $\mathbb{P}$. The second-stage vectors x_2^s have components $(x_2^+(\xi), x_2^-(\xi)) \in \mathbb{R}^2$, with respective scalar costs F_2^+ and F_2^-, satisfying $F_2^- \geqslant F_2^+ > 0$. We furthermore take $b_1\,, b_2 = +\infty$, $x_1 \in \mathbb{R}$ and let $T = 1$, $W = [1 - 1]$ so that the optimization problem is

$$\begin{cases} \min & F_1 x_1 + \mathbb{E}[F_2^+ x_2^+(\xi) + F_2^- x_2^-(\xi)] & \\ \text{s.t.} & x_1 \geqslant 0 & \\ & x_2^+(\xi) \geqslant 0\,, x_2^-(\xi) \geqslant 0 & \text{for a.e. } \xi \\ & x_1 + x_2^+(\xi) - x_2^-(\xi) = \xi & \text{for a.e. } \xi\,, \end{cases}$$

with $F_1 > 0$ and where the feasible set is assumed not empty for a.e. ξ. Rewriting this problem in a two-level formulation,

$$\begin{cases} \min & F_1 x_1 + \mathbb{E}[Q(x_1,\xi)] \\ \text{s.t.} & x_1 \geqslant 0 \end{cases} \quad , \quad Q(x_1,\xi) := \begin{cases} \min & F_2^+ x_2^+ + F_2^- x_2^- \\ \text{s.t.} & x_2^+, x_2^- \geqslant 0 \\ & x_2^+ - x_2^- = \xi - x_1 \end{cases} \tag{4}$$

gives, by Linear Programming duality, that

$$Q(x_1,\xi) := \begin{cases} \max & \pi(\xi - x_1) \\ \text{s.t.} & -F_2^- \leqslant \pi \leqslant F_2^+ \,. \end{cases}$$

Therefore, the optimal multiplier associated with the affine constraint in (4) is

$$\pi(x_1,\xi) := \begin{cases} -F_2^- & \text{if } \xi - x_1 < 0 \\ \text{any element in } [-F_2^-, F_2^+] & \text{if } \xi - x_1 = 0 \\ F_2^+ & \text{if } \xi - x_1 > 0\,. \end{cases} \tag{5}$$

The recourse function can be written

$$Q(x_1,\xi) = F_2^- \max(x_1 - \xi, 0) + F_2^+ \max(\xi - x_1, 0),$$

yielding an explicit form for the expected value

$$\mathbb{E}[Q(x_1,\xi)] = F_2^- \mathbb{P}(\xi \leqslant x_1) + F_2^+ \mathbb{P}(\xi \geqslant x_1) = F_2^+ + (F_2^- - F_2^+)\mathbb{P}(\xi \leqslant x_1)\,,$$

and problem (4) boils down to

$$\min_{x_1 \geqslant 0} F_1 x_1 + \mathbb{E}[Q(x_1,\xi) = F_2^+ + \min_{x_1 \geqslant 0} F_1 x_1 + (F_2^- - F_2^+)\mathbb{P}(\xi \leqslant x_1)\,.$$

The cumulative distribution $\mathbb{P}(\xi \leqslant \cdot)$ is a non-decreasing function. Since, in addition, $F_1 > 0$ and $F_2^- \geqslant F_2^+$ by assumption, the minimizer is $\bar{x}_1 = 0$. The corresponding optimal price distribution is

$$\bar{\pi}(\xi) = \begin{cases} -F_2^- & \text{if } \xi < 0 \\ \text{any element in } [-F_2^-, F_2^+] & \text{if } \xi = 0 \\ F_2^+ & \text{if } \xi > 0\,. \end{cases}$$

For simplicity, let $F_2^- = F_2^+ = F_2$ and suppose that ξ has a symmetric probability distribution $\mathbb{P}$. Then the continuous price signal for (4) has mean and variance

$$\mathbb{E}[\bar{\pi}(\xi)] = 0 \quad \text{and} \quad \mathbb{V}ar[\bar{\pi}(\xi)] = \mathbb{E}[\bar{\pi}(\xi)^2] = F_2^2\,. \tag{6}$$

If the problem arises in a company with Manager 1 sampling only negative numbers while Manager 2 samples only positive numbers, then $S_1 \subset \mathbb{R}_-$ and $S_2 \subset \mathbb{R}_+$ will respectively result in

$$\begin{array}{lllll} \forall s \in \mathbb{S}_1 & \bar{\pi}_1(\xi^s) = -F_2 & \Longrightarrow & \mathbb{E}[\bar{\pi}_1] = -F_2 \quad \text{and} & \mathbb{V}ar[\bar{\pi}_1] = 0 \\ \forall s \in \mathbb{S}_2 & \bar{\pi}_2(\xi^s) = F_2 & \Longrightarrow & \mathbb{E}[\bar{\pi}_2] = F_2 \quad \text{and} & \mathbb{V}ar[\bar{\pi}_2] = 0\,. \end{array} \tag{7}$$

These are very different (and wrong) empirical signals, no matter how large the samples are.

Of course, this example illustrates an extreme case and any intermediate situation between the most wrong one (as above) and "right" ones (with S_1 and S_2 containing the same number of positive and negative numbers) are possible. It is undeniable that the sampling method has an impact in reducing variance. Nevertheless, the stochastic nature of the energy problem (2) still remains, making the issue of producing reliable price signals a real concern for decision makers.

3.2 Dual Regularization of Two Stage Problems

We now extend to the box-constrained setting the stabilization device proposed in [12], to obtain multipliers with minimum norm.

Like for the simple example, consider the two-level reformulation of (2),

$$\begin{cases} \min & \langle F_1, x_1\rangle + \sum_{s\in\mathbb{S}} p^s Q^s(x_1) \\ \text{s.t.} & 0 \leqslant x_1 \leqslant b_1\,, \end{cases} \tag{8}$$

making use of the following recourse function, once more given in primal and dual forms:

$$Q^s(x_1) := \begin{cases} \min & \langle F_2, x_2\rangle \\ \text{s.t.} & 0 \leqslant x_2 \leqslant b_2 \\ & Wx_2 = h^s - Tx_1 \end{cases} = \begin{cases} \max & \langle \pi, h^s - Tx_1\rangle - \langle \lambda, b_2\rangle \\ \text{s.t.} & -\lambda + W^\top \pi \leqslant F_2 \\ & \lambda \geqslant 0\,. \end{cases} \tag{9}$$

Stability of the dual variables is achieved by considering the following regularized recourse functions, depending on a parameter $\beta > 0$,

$$Q^{\beta,s}(x_1) := \begin{cases} \max & \langle \pi, h^s - Tx_1\rangle - \langle \lambda, b_2\rangle - \frac{\beta}{2}\|\pi\|^2 \\ \text{s.t.} & -\lambda + W^\top \pi \leqslant F_2 \\ & \lambda \geqslant 0\,. \end{cases} \tag{10}$$

By construction, the maximizer $\bar\pi^{\beta,s}(x_1)$ is unique. Using once again duality,

$$Q^{\beta,s}(x_1) = \begin{cases} \min & \langle F_2, x_2\rangle + \frac{1}{2\beta}\|h^s - Wx_2 - Tx_1\|^2 \\ \text{s.t.} & 0 \leqslant x_2 \leqslant b_2\,, \end{cases}$$

whose solutions $\bar x_2^{\beta,s}(x_1)$ define a *proxy* for the multiplier π:

$$\bar\pi^{\beta,s}(x_1) = \frac{h^s - Wx_2^{\beta,s}(x_1) - Tx_1}{\beta}. \tag{11}$$

Notice that neither the λ-components solving (10) nor the second-stage primal minimizers $\bar x_2^{\beta,s}(x_1)$ are guaranteed to be unique. Also, with respect to [12], the upper bounds in our setting introduce the multiplier λ, that was not present in that work.

Going back to the one-level formulation, instead of the linear program (2), we shall solve a quadratic programming problem of the form

$$\begin{cases} \min & \langle F_1, x_1\rangle + \sum_{s\in\mathbb{S}} p^s \Big(\langle F_2, x_2^s\rangle + \frac{1}{2\beta}\Big\| h^s - Wx_2^s - Tx_1 \Big\|^2 \Big) \\ \text{s.t.} & 0 \leqslant x_1 \leqslant b_1 \\ & 0 \leqslant x_2^s \leqslant b_2 \quad \text{for } s \in \mathbb{S}\,. \end{cases} \tag{12}$$

With respect to our energy management problem (2), the rightmost term in the objective function above (with factor $\frac{1}{\beta}$) corresponds to relaxing the water balance equations. These are very important constraints for long term optimal energy management problems. In our numerical experiments in Section 4, for the Nordic energy system, the value of β is chosen so that the total violation is smaller than 1% of the whole hydro-capacity, see Figures 5 and 6.

3.3 Back to the analytical case

The effects of our regularization can be examined for the illustrative problem from Section 3. For a symmetric probability distribution and $F_2^- = F_2^+ = F_2$, the stabilized version of (4) is

$$\begin{cases} \min & F_1 x_1 + E[Q^\beta(x_1, \xi)] \\ \text{s.t.} & x_1 \geqslant 0\,, \end{cases} \quad \text{for } Q^\beta(x_1,\xi) = \begin{cases} \max & (\xi - x_1)\pi - \dfrac{\beta}{2}\pi^2 \\ & -F_2 \leqslant \pi \leqslant F_2\,, \end{cases} \tag{13}$$

which yields a proxy multiplier

$$\pi^{\beta}(x_1,\xi) := \begin{cases} -F_2 & \text{if } \xi - x_1 < -\beta F_2 \\ \dfrac{\xi - x_1}{\beta} & \text{if } \xi - x_1 \in [-\beta F_2, \beta F_2] \\ F_2^+ & \text{if } \xi - x_1 > \beta F_2\,, \end{cases} \tag{14}$$

to be compared with the multipliers (5), explicitly computed for the initial problem.

Continuing with the actions of our two managers, now solving the regularized problems, suppose β_k is sufficiently large for the inequality $x_1^k - \beta_k F_2 < 0$ to hold. Even if Manager 1 still samples only negative numbers, now the set S_1 may contain scenarios for which $\xi^s - x_1^k \in [-\beta_k F_2, 0]$, with prices possibly larger than $-F_2$. Similarly, now Manager 2 can sample $\xi^s \in [0, x_1^k + \beta_k F_2]$ for some $s \in \mathbb{S}_2$, thus also considering prices smaller than F_2 when computing the mean. It is therefore likely that the empirical expected prices will be closer to the true mean.

The result below formalizes this assertion. Recall from (6) that the moments for the price signal at the solution $\bar{x}_1 = 0$ are

$$\mathbb{E}[\bar{\pi}(\xi)] = 0 \quad \text{and} \quad \mathbb{V}\mathrm{ar}[\bar{\pi}(\xi)] = F_2^2\,.$$

Proposition 3.1. *Consider the simple problem* (4)*, with minimizer* $\bar{x}_1 = 0$ *and let* $\bar{\pi}(\xi)$ *be an optimal multiplier associated with the affine constraint in the recourse function* $Q(\bar{x}_1,\xi)$*. The following holds for* $\left(x_1^k, \pi^k(\xi) = \pi^{\beta_k}(x_1^k,\xi)\right)$ *solving the regularized problem* (13)*, written with* $\beta = \beta_k$*:*

$$\lim_{\beta_k \to 0} \mathbb{E}[\pi^k(\xi)] = \mathbb{E}[\bar{\pi}(\xi)] \quad \textit{with} \quad \mathbb{V}\mathrm{ar}[\pi^k(\xi)] \leqslant \mathbb{V}\mathrm{ar}[\bar{\pi}(\xi)]\,. \tag{15}$$

Proof. It is convenient to introduce the short notation

$$\Gamma_-^k := \mathbb{P}(\xi - x_1^k \leqslant -\beta_k F_2)\,, \text{ and } \Gamma_+^k := \mathbb{P}(\xi - x_1^k \geqslant \beta_k F_2)\,,$$

noting that, by the symmetry assumption and the fact that $x_1^k \to \bar{x} = 0$,

$$\lim_{\beta_k \to 0} \Gamma_+^k = \mathbb{P}(\xi \geqslant 0) = \frac{1}{2} = \mathbb{P}(\xi \leqslant 0) = \lim_{\beta_k \to 0} \Gamma_-^k\,. \tag{16}$$

The average of prices (14) is

$$\mathbb{E}[\pi^k(\xi)] = F_2(\Gamma_+^k - \Gamma_-^k) + \int_{x_1^k - \beta_k F_2}^{x_1^k + \beta_k F_2} \frac{\xi - x_1^k}{\beta_k} d\xi\,.$$

To compute the limit, first bound the integral as follows:

$$-\Gamma^k F_2 \leqslant \int_{x_1^k - \beta_k F_2}^{x_1^k + \beta_k F_2} \frac{\xi - x_1^k}{\beta_k} d\xi \leqslant \Gamma^k F_2\,,$$

for

$$\Gamma^k := \mathbb{P}(-\beta_k F_2 \leqslant \xi - x_1^k \leqslant \beta_k F_2)\,.$$

Then, using that $\lim_{\beta_k \to 0} \Gamma^k = 0$, passing to the limit as $\beta_k \to 0$ in the inequalities below

$$F_2(\Gamma_+^k - \Gamma_-^k - \Gamma^k) \leqslant \mathbb{E}[\pi^k] \leqslant F_2(\Gamma_+^k - \Gamma_-^k + \Gamma^k)\,, \tag{17}$$

yields, together with (16), that $\lim_{\beta_k \to 0} \mathbb{E}[\pi^k] = 0$, as claimed.

To get the variance expression, since $\mathbb{V}\mathrm{ar}[\pi] = \mathbb{E}[\pi^2] - \mathbb{E}[\pi]^2$, we first compute the term

$$\mathbb{E}[\pi^k(\xi)^2] = F_2^2(\Gamma_+^k - \Gamma_-^k) + \int_{x_1^k - \beta_k F_2}^{x_1^k + \beta_k F_2} \frac{(\xi - x_1^k)^2}{\beta_k^2} d\xi \,,$$

and bound again the integral, as follows:

$$-\Gamma^k F_2^2 \leqslant \int_{x_1^k - \beta_k F_2}^{x_1^k + \beta_k F_2} \frac{(\xi - x_1^k)^2}{\beta_k^2} d\xi \leqslant \Gamma^k F_2^2 \,.$$

Adding the negative of (17) gives

$$F_2(\Gamma_+^k - \Gamma_-^k - \Gamma^k) \leqslant \mathbb{E}[\pi^k(\xi)^2] - \mathbb{E}[\pi^k] F_2(\Gamma_+^k - \Gamma_-^k + \Gamma^k) \,.$$

Since $\mathbb{V}\mathrm{ar}[Z] = \mathbb{E}[Z^2] - \mathbb{E}[Z]^2$ for any random variable Z, this means that

$$F_2(\Gamma_+^k - \Gamma_-^k - \Gamma^k) \leqslant \mathbb{V}\mathrm{ar}[\pi^k] \leqslant F_2(\Gamma_+^k - \Gamma_-^k + \Gamma^k) \,.$$

Then, passing to the limit as $\beta_k \to 0$, gives the desired result. □

The positive impact of the regularization is shown numerically in Figure 3 below. We consider a normal distribution $\xi \sim \mathcal{N}(0, 10)$, $F_2 = F_1 = 5$, and samples $\Xi = \{\xi^1, \ldots, \xi^{\mathbb{S}}\}$ with $S = 200$ elements. We fix $\beta = 1$, and compute the numerical value for the multipliers $\bar{\pi}$ and $\bar{\pi}^\beta$ given in (5) and (14). The respective histograms are shown in Figure 2.

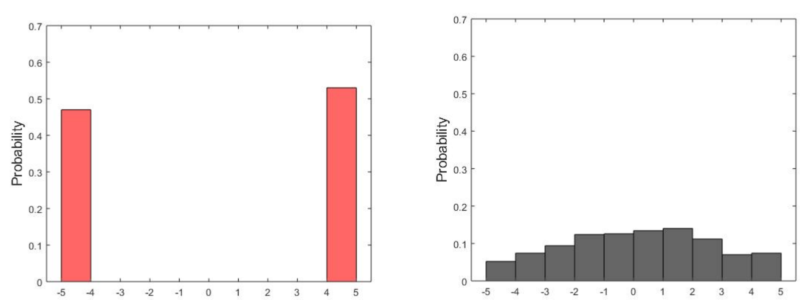

Figure 2: Non-regularized (left) and regularized (right) price signal distributions

The histograms are consistent with the theory: on the left, the values of $\bar{\pi}$ oscillate between -5 and 5, (that is, $-F_2$ and F_2); on the right, the distribution of $\bar{\pi}^\beta$ looks smoother.

To see the impact of regularization on the expected value and variance we repeated the same test with different samples Ξ^n, $n \in \{1, \ldots, N\}$ for $N = 40$.

The distribution of $\bar{\pi}^\beta$ is computed using $\bar{x}_1^\beta$, the regularized primal solution for the one-level regularized problem (13). The expected value and variance for the $N = 40$ samples are reported in Figure 3.

Clearly, results cannot match exactly the theoretical ones because we are using a finite sample, instead of the continuous normal distribution. Notwithstanding, the left plot in Figure 3 confirms that the expected value is around zero, with the non-regularized model exhibiting a higher variability. On the right plot, on the other hand, we see that when $\beta = 0$ the variance indeed stays close to $25 = 5^2 = F_2^2$, being significantly smaller for the regularized model.

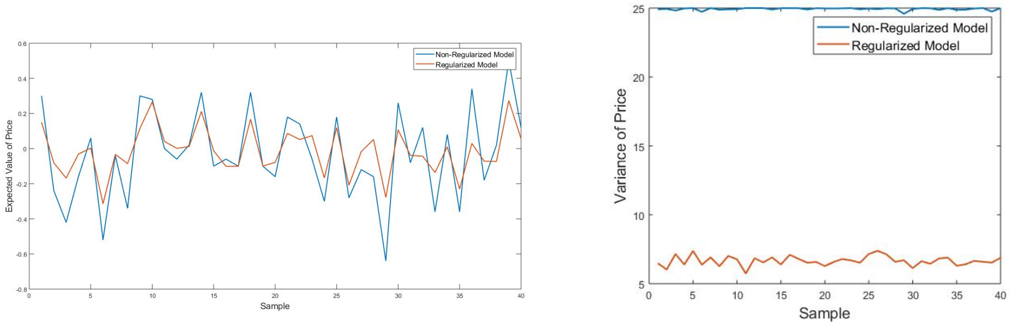

Figure 3: Expected value and variance for 40 samples

3.4 Asymptotic properties of the dual regularization

By the convergence theory in [12], as $\beta \to 0$, the proxy multiplier converges to the multiplier of the original problem that has minimal norm. That work considers more general quadratic objective functions, including possibly nonconvex but, as already mentioned, [12] only deals with equality and nonnegativity (thus, lower bound) constraints. We show how to adapt the theory for problems with upper bounds as in (2). Basically, the results from [12] can be in some instances specialized, and in other instances slightly extended, to the current setting.

To cast (2) and (12) in the the setting of [12], suppose the scenario set is $\mathbb{S} := \{1, \dots, S\}$ denote by n_1 and n_2 the respective dimensions of x_1, x_2^s defined in (3). We define the vectors

$$x := (x_1, x_2^1, \dots, x_2^S) \in \mathbb{R}^n \,, \text{ where } n := n_1 + n_2 S \,,$$

$$g := (F_1, p^1 F_2, \dots, p^S F_2) \in \mathbb{R}^n \,,$$

$$a := (h^1, \dots, h^S) \in \mathbb{R}^{mS} \,, b := (b_1, b_2, \dots, b_2) \in \mathbb{R}^n \,.$$

and the $mS \times n$ matrix

$$A := \begin{bmatrix} T & W & 0 & \dots & 0 \\ T & 0 & W & \ddots & \vdots \\ T & \vdots & \ddots & \ddots & 0 \\ T & 0 & \dots & 0 & W \end{bmatrix} , \tag{18}$$

where m is the dimension of h^s. With this notation, problem (2) becomes

$$\begin{cases} \min & \langle g, x \rangle \\ \text{s.t.} & Ax = a \\ & 0 \leqslant x \leqslant b \,. \end{cases} \tag{19}$$

The multiplier associated with the constraint $Ax = a$ in (19) is denoted π, while the box-constraint multipliers are denoted by μ and λ, respectively for the lower and upper bounds. The convergence results for our regularization are given below.

Theorem 3.2 (Primal and dual convergence in the setting of problem (19))**.**
Consider the penalization problem (12)*, which writes down as*

$$\begin{cases} \min & \langle g, x \rangle + \frac{1}{2\beta} \|Ax - a\|^2 \\ s.t. & 0 \leqslant x \leqslant b \,, \end{cases} \tag{20}$$

Let the triplet (x^k, μ^k, λ^k) *denote the optimal primal and dual solutions (Lagrange multipliers) to* (20), *written with* $\beta = \beta_k$, *and let* $\pi^k := (Ax^k - a)/\beta_k$.

If $\beta_{k+1} < \beta_k$ *for all* k, *and* $\beta_k \to 0$, *the following holds:*

(i) *The primal sequence* $\{x^k\}$ *is bounded and any of its accumulation points minimizes* (19).

(ii) *Let* $\{x^{k_j}\} \to \bar{x}$ *as* $j \to \infty$ *and let* $N_{\{0 \leqslant x \leqslant b\}}(\bar{x})$ *denote the cone normal to the box-constraints at* $\bar{x}$. *If the condition*

$$\mathrm{Im}(A^\top) \cap N_{\{0 \leqslant x \leqslant b\}}(\bar{x}) = \{0\} \tag{21}$$

holds, then $\{\mu^{k_j}\}$ *and* $\{\lambda^{k_j}\}$ *are bounded. Moreover, for any accumulation point* $(\bar{\mu}, \bar{\lambda})$ *of the subsequence* $\{(\mu^{k_j}, \lambda^{k_j})\}$, *the corresponding subsequence* $\{\pi^{k_j}\}$ *converges to* $\hat{\pi}$, *the solution of:*

$$\min \frac{1}{2}\|\pi\|^2 \, s.t. \quad g + A^\top \pi - \bar{\mu} + \bar{\lambda} = 0. \tag{22}$$

The point $(\bar{x}, \hat{\pi}, \bar{\mu}, \bar{\lambda})$ *is a primal-dual solution of* (19).

Proof. Item (i) is immediate: Every sequence $\{x^k\}$ generated by the method is automatically bounded (and thus has a convergent subsequence), because the set $X = \{0 \leqslant x \leqslant b\}$ is compact. Then, every accumulation point of $\{x^k\}$ is a solution of (19), by [12, Thm. 3.4].

We proceed to item (ii). By KKT conditions for (20), we have that

$$\begin{gathered} g + \frac{1}{\beta_k} A^\top (Ax^k - a) - \mu_0^k + \mu_b^k = 0, \\ x^k \geqslant 0, \ \mu_0^k \geqslant 0, \ \langle \mu_0^k, x^k \rangle = 0, \quad x^k \leqslant b, \ \mu_b^k \geqslant 0, \ \langle \mu_b^k, x^k - b \rangle = 0. \end{gathered} \tag{23}$$

Recalling the definition of π^k and setting $\mu^k := \mu_b^k - \mu_0^k$, we obtain that

$$g + A^\top \pi^k + \mu^k = 0. \tag{24}$$

Let $\{x^{k_j}\} \to \bar{x}$ as $j \to \infty$. We next prove that the sequence $\{(\mu_0^{k_j}, \mu_b^{k_j})\}$ is bounded. To that end, using the second line in (23), first observe the following:

$$\begin{gathered} (\mu_0^k)_i > 0 \ \Rightarrow \ x_i^k = 0 \ \Rightarrow \ (\mu_b^k)_i = 0, \ \mu_i^k = -(\mu_0^k)_i < 0, \\ (\mu_b^k)_i > 0 \ \Rightarrow x_i^k = b \ \Rightarrow (\mu_0^k)_i = 0, \ \mu_i^k = (\mu_b^k)_i > 0. \end{gathered} \tag{25}$$

From those relations, it is obvious that $\{(\mu_0^{k_j}, \mu_b^{k_j})\}$ is bounded if and only if $\{\mu^{k_j}\}$ is bounded.

Next, similarly to the proof of [12, Thm. 3.4], suppose by contradiction that (23) (and thus (24)) hold with $\|\mu^{k_j}\| \to +\infty$. Passing onto a subsequence, if necessary, let $\{\mu^{k_j}/\|\mu^{k_j}\|\} \to \bar{\mu} \neq 0$. Denote $u^{k_j} = -A^\top \pi^{k_j}/\|\mu^{k_j}\| \in \mathrm{Im}\, A^\top$. Dividing the equality in (24) by $\|\mu^{k_j}\|$ and passing onto the limit as $j \to \infty$, it follows that

$$u^{k_j} = (g + \mu^{k_j})/\|\mu^{k_j}\| \to \bar{\mu} \neq 0.$$

As $u^{k_j} \in \mathrm{Im}\, A^\top$, $u^{k_j} \to \bar{\mu}$, and $\mathrm{Im}\, A^\top$ is closed, we conclude that $\bar{\mu} \in \mathrm{Im}\, A^\top$.

Observe now that from (25) it follows that

$$\bar{\mu}_i < 0 \ \Rightarrow \ \bar{x}_i = 0 \quad \text{and} \quad \bar{\mu}_i > 0 \ \Rightarrow \ \bar{x}_i = b.$$

This shows that $\bar{\mu} \in N_X(\bar{x})$. As $\bar{\mu} \neq 0$ and $\bar{\mu} \in \mathrm{Im}\, A^\top$, we obtain a contradiction with (21). It follows that $\{\mu^{k_j}\}$ is bounded. And as already observed from (25), this means that $\{\mu_0^{k_j}\}$ and $\{\mu_b^{k_j}\}$ are bounded. The proof that the corresponding subsequence $\{\pi^{k_j}\}$ converges to $\hat{\pi}$, the solution of (22), is analogous to that in Theorem [12, Thm. 3.4].

□

Some comments are in order about the relations between the statements in Theorem 3.2 and those in Theorems 3.3 and 3.4 in [12]. The fact that all accumulation points of $\{x^k\}$ are solutions to (19) is a standard property of exterior penalty methods, see [12, Thm. 3.1] and accompanying comments. However, the *existence* of accumulation points (i.e., boundedness of $\{x^k\}$) is not automatic. In [12, Thm. 3.3], boundedness of the primal sequence was established under certain assumptions. Note that in the current setting we do not need any assumptions, as (20) has box-constraints (and so its feasible set is compact). Condition (21) can be interpreted as a *partial* Mangasarian–Fromovitz condition; see [12, Thm. 2.1] and the associated comments. Its role is to ensure boundedness of the multipliers associated to box-constraints, while allowing the set of multipliers associated to the equality constraints to be unbounded (and in particular, allow for the matrix A to be not of full rank).

4 Benchmark for Northern European system

The energy system described in Section 2 has 12 bidding zones. Norway, with 5 zones, has the largest percentage of hydro-energy generation, which amounts to an equivalent of 95% of its demand. Other countries have several different sources of energy, Sweden has a large proportion of nuclear generation, while in Denmark wind generation amounted to half of its demand in 2014. As in the diagram in Figure 1, imports and exports are handled as interconnections between zones. In total the system has $\mathbb{L} = 30$ balancing zones, $\mathbb{J} = 21$ hydro-power plants, and $\mathbb{I} = 224$ thermal power plants. Hydro-power plants are assumed to have no generation cost. Our model uses real and estimated values from ENGIE's database for historical inflows, thermal generation and import costs, capacity of each power plant in the system, minimum and maximum level of reservoirs and maximum flow between zones. Finally, the inflow uncertainty was generated by calibrating a log-normal distribution over historical inflow scenarios.

As usual with multi-stage stochastic programs, the numerical assessment is split into two steps. One defining implementable policies by solving the multi-stage energy problem, and a second phase, simulating the system operation under the policy provided as an output of the optimization step.

4.1 Optimization Phase

Our goal is to compare the price signals obtained by SDDP on the original multi-stage problem with our two-stage regularized approach running in a rolling-horizon mode, denoted below by RRH. A third solver, RH, is the two-stage rolling-horizon algorithm without regularization. The mechanism of rolling horizon put in place for both RH and RRH is described below.

4.1.1 Rolling-horizon Methodology

The time horizon of one year was discretized in $t = 1, \dots, 8760$ hours. At the first hour of each week, the inflow uncertainty of the whole week becomes known. Since the year has 54 weeks, this defines a multi-stage structure of uncertainty, that we cast in our two-stage setting as follows.

We put in place a *rolling-horizon* mode, in which we solve $w = 1, \dots, 53$ two-stage problems derived from (1) in Section 2. In the w-th two-stage problem, the decision variables of the w-th week are considered in the first stage. The uncertainty of the remaining $w+1, \dots, 54$ weeks is revealed at once, at the end of the week w and, hence, the corresponding decision variables are considered in the second stage. Since one week has 168 hours, the time horizon of the w-th problem covers $\mathbb{T}^w := (54 - w + 1)168$ hours. The output of the w-th two-stage problem provides input for the problem $w+1$, similarly to [6].

With this mechanism, the first-stage components of the decision vector of problem w are in fact decision variables for the w-th week. Accordingly, if $\bar{x}_1^{\beta;w}$ denotes the first-stage component of a solution obtained for the w-th two-stage problem, then the primal policy

$$\left\{\bar{x}_1^{\beta;w} : w = 1, \dots, 52\right\} \tag{26}$$

is *implementable*, or nonanticipative, as defined in [21]. Another output, close to SDDP pricing mechanism, is the following dual policy, also implementable, that gives a value to water:

$$\left\{ \text{ the cuts for } \mathbb{E}\left[Q^{\beta,s;w}(\bar{x}_1^{\beta;w})\right] ; w = 1, \dots, 53\right\} . \tag{27}$$

that is, the cuts of the successive expected recourse functions at a solution.

We now define mathematically the problem solved in a rolling horizon. In the next sections we shall use this formulation as a reference to explain our simulations.

Following the notation introduced in section 2 to formulate the energy management problem, for the w-th week we let

$$\mathbb{T}_w = \{t \ : \ 7(w-1) < t \leqslant 7w\}, \text{ and } A_w = \{t \ : \ 7w < t\}.$$

We write the problem for the w-th week as follows:

$$\left\{\begin{array}{lll} \min & \displaystyle\sum_{t\in\mathbb{T}_w}\sum_{l\in\mathbb{L}}\sum_{i\in\mathbb{I}_l} C_i^t gt_i^t + \mathbb{E}[\mathbb{Q}_w^\beta(v_j^{7w}, \mathcal{I}_j^s)] & \\ \text{s.t.} & \underline{v}_j^t \leqslant v_j^t \leqslant \overline{v}_j^t \text{ and } 0 \leqslant sp_j^t, & j\in\mathbb{J}_l, l\in\mathbb{L}, t\in\mathbb{T}_w \\ & 0 \leqslant gh_j^t \leqslant \overline{gh}_j^t, \quad \underline{0 \leqslant gt}_i^t \leqslant \overline{gt}_i^t, & j\in\mathbb{J}_l, i\in\mathbb{I}_l, l\in\mathbb{L}, t\in\mathbb{T}_w \\ & -\underline{f_{l\leftrightarrow l_1}^t} \leqslant f_{l\leftrightarrow l_1}^t \leqslant \overline{f_{l\leftrightarrow l_1}^t}, & l\in\mathbb{L} : l_1\in\mathbb{F}_l \neq \emptyset, t\in\mathbb{T}_w \\ & v_j^t - v_j^{t-1} + gh_j^t + sp_j^t = \mathcal{I}_j^t, & j\in\mathbb{J}_l, l\in\mathbb{L}, t\in\mathbb{T}_w \\ & \displaystyle\sum_{j\in\mathbb{J}_l} gh_j^t + \sum_{i\in\mathbb{I}_l} gt_i^t + \sum_{l_1\in\mathbb{F}_l\neq\emptyset} f_{l\leftrightarrow l_1}^t = \mathcal{D}_l^t, & l\in\mathbb{L}, t\in\mathbb{T}_w . \end{array}\right.$$

where $v_j^{7(w-1)}$ is the reservoir level decision that had been made in the $(w-1)$-th week. Here, $\mathcal{I}_j^t$ is random, but it does not depend on the scenario s. The sequence $(\mathcal{I}_{j,w}^t)$, where $t \in \mathbb{T}_w$ is a path in the tree of scenarios.

The regularized recourse functions defined in the second stage are

$$\mathbb{Q}_w^\beta(v_j^{7w}, \mathcal{I}_j^s) :=$$

$$\left\{\begin{array}{llll} \min & \displaystyle\sum_{t\in A_w}\sum_{l\in\mathbb{L}}\sum_{i\in\mathbb{I}_l} C_i^t gt_i^t \quad + \frac{1}{2\beta}\|v_j^{7n+1} - v_j^{7w} + gh_j^{7w+1} + sp_j^{7w+1} - \mathcal{I}_j^{7w+1,s}\|^2 & & \\ \text{s.t.} & \underline{v}_j^t \leqslant v_j^t \leqslant \overline{v}_j^t \text{ and } 0 \leqslant sp_j^t, & j\in\mathbb{J}_l, l\in\mathbb{L}, & t\in A_w \\ & 0 \leqslant gh_j^t \leqslant \overline{gh}_j^t, \quad \underline{0 \leqslant gt}_i^t \leqslant \overline{gt}_i^t, & j\in\mathbb{J}_l, i\in\mathbb{I}_l, l\in\mathbb{L}, & t\in A_w \\ & -\underline{f_{l\leftrightarrow l_1}^t} \leqslant f_{l\leftrightarrow l_1}^t \leqslant \overline{f_{l\leftrightarrow l_1}^t}, & l\in\mathbb{L} : l_1\in\mathbb{F}_l \neq \emptyset, & t\in A_w \\ & v_j^t - v_j^{t-1} + gh_j^t + sp_j^t = \mathcal{I}_j^{t,s} \ \leftrightarrow \pi_j^{t,s}, & j\in\mathbb{J}_l, l\in\mathbb{L}, , & t\in A_w \\ & \displaystyle\sum_{j\in\mathbb{J}_l} gh_j^t + \sum_{i\in\mathbb{I}_l} gt_i^t + \sum_{l_1\in\mathbb{F}_l\neq\emptyset} f_{l\leftrightarrow l_1}^t = \mathcal{D}_l^t, & l\in\mathbb{L}, & t\in A_w , \end{array}\right.$$

where $\mathcal{I}_j^{t,s}$ is random and depends on the scenario s. When $\beta = 0$, the constraint moves from the objective function to the feasible set.

In this notation the sequence $\left\{\bar{x}_1^{\beta;w} : w = 1, \dots, 52\right\}$ from (26) corresponds to the reservoir level $\bar{x}^{\beta;w} = (v_j^{7w})$, while the cuts for the function $\mathbb{E}\left[Q^{\beta,s;w}(\bar{x}_1^{\beta;w})\right]$ in (27) are expressed in terms of the couple $(\bar{\pi}_{j,k}^{7w+1}, \delta_{it}^w)$, for each iteration k, where $\bar{\pi}_k^{7n+1,k} > 0$, and:

$$\bar{\pi}_{j,it}^{7w+1,k} = \frac{1}{S}\sum_{s} \pi_{j,it}^{7w+1,k,s},$$

$$\delta_k^w = \frac{1}{S}\sum_{s} \mathbb{Q}_{w,k}(v_j^{7w}, \mathcal{I}^s) - \sum_{j} \bar{\pi}_{j,k}^{7w+1,k} v_j^{7w}.$$

We note that the regularized problem above differs slightly from the abstract formulation (2). The latter includes in the penalization, via the definitions of T and W, both the water balance and demand constraints. In the problem above, by contrast, we only penalize the water balance, to simplify the implementation. For these problems, if the reservoir levels are kept below their maximal capacity, the Lagrange multipliers of the demand and water balance equation coincide (in the figures below, with the reservoir dynamics after the optimization and simulation phases, the maximum capacity is never reached).

4.1.2 Results for the optimization phase

The optimization part of the experiment uses an in-sample set with 30 inflow scenarios and takes $\beta := 7000$ for RRH (below we explain that with this value, the magnitude of the violation incurred by RRH is less then 1% for the whole system). The SDDP method takes one scenario randomly in the forward pass and all the 30 scenarios in the backward pass. The rolling-horizon variants take the same forward scenario, for the different weeks $w = 1, 2, \ldots$, including the 30 scenarios from week $w + 1$ to week 48 in the second stage of the w-th two-stage problem.

The aggregate reservoir management (adding all the hydro-plants), is shown in Figure 4, where colors correspond to the different weeks. The values are normalized with respect to the maximum system capacity.

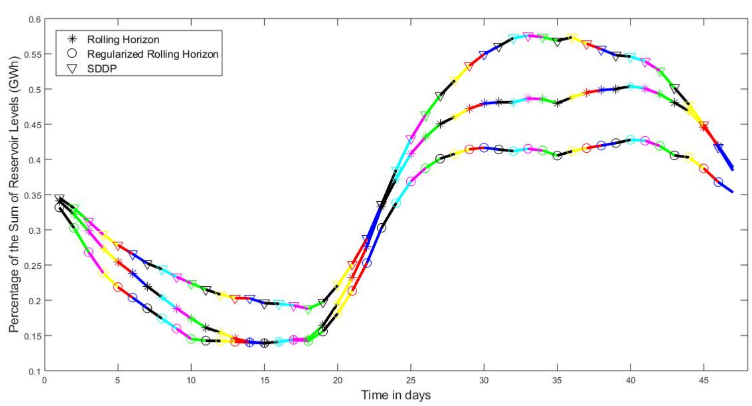

Figure 4: Aggregate reservoir management - optimization phase

It is important to explain that the SDDP curve was made running the SDDP algorithm and storing cuts, that estimate the future cost function, until SDDP converges. Having these cuts as input, we then ran a forward path of SDDP following the same path considered by RH and RRH, making a fair comparison between these tree models.

The levels of reservoirs with the rolling-horizon modes are lower, with the RRH using the most of water. Since SDDP sees a larger portion of the scenario tree in the backward pass (not only the tail of the weeks $w + 1, \ldots, 54$), SDDP water management is more conservative. Regarding the comparison between RRH and RH, note that the inequality $Q^{\beta,s}(\cdot) \leqslant Q^s(\cdot)$ always holds (the feasible set defining the former is included in the one defining the latter). Having an under-estimation of the future-cost function, RRH tends to be less conservative than RH, keeping less water in the reservoirs.

Since RRH does not consider the water-balance equations, in Figure 5 we examine the gap

$$v_j^t - v_j^{t-1} + gh_j^t + sp_j^t - \mathcal{I}_j^{t,s}$$

over the first 48 weeks for $s = 1, \ldots, 12$ scenarios (different colors in the figure), for two hydro-plants in Norway.

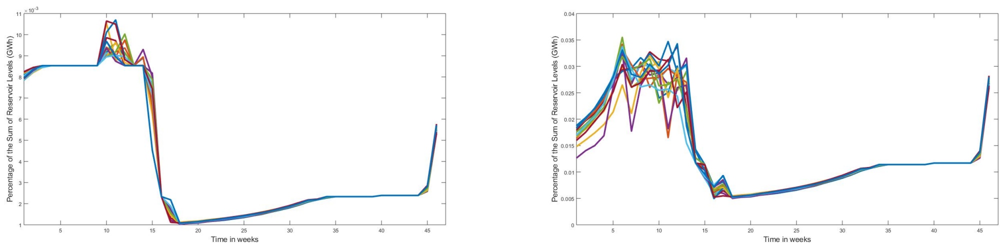

Figure 5: Absolute violation of water balance - Hydro-plants 1 and 3 in Norway (left and right)

We note that the system exploits the most the possibility of not satisfying the water-balance equation in the beginning of the year, when inflows are smaller. In order to determine the real extent of the violation, relative to the total hydro-capacity, we use the expression for the multiplier proxy

$$\pi^\beta(\xi) = \frac{Tx_1 + Wx_2(\xi) - h(\xi)}{\beta},$$

to estimate the gap by $\beta\pi^\beta(\xi)$. Since $\beta = 7000$ and the price signals are about 10^2, the magnitude of the violation incurred by RRH is of order 10^5. This is consistent with the graphs in Figure 5. The whole hydro-capacity being about 10^7, the gap is less then 1% for the whole system. The mean violation, in relative values, over the 30 scenarios and all the hydro-power plants, is shown in Figure 6 for the first 48 weeks.

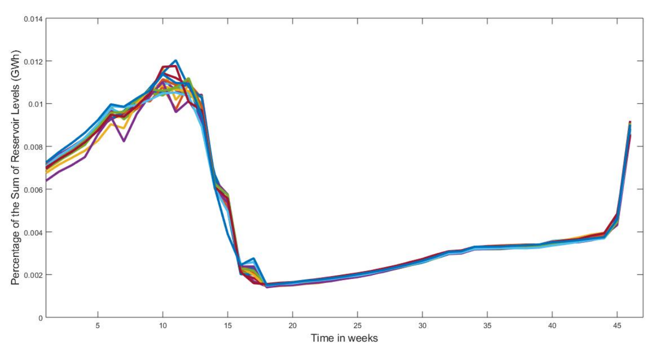

Figure 6: Relative mean violation of water balance in the whole system

4.2 Simulation phase

We now assess the quality of the policies obtained by the three solvers on an out-of-sample set with 200 scenarios. After the optimization phase, we simulate different scenarios as input data and examine the Wasserstein distance between the histograms of the respective price signals, [23]. We expect to obtain similar expected values for the three solvers, but a smoother distribution for RRH. A similar measure for the quality of optimal decisions is considered in [9], to assess a proposal to build a scenario tree that preserves certain essential statistical properties. The different trees generated with their approach maintain the optimal value of the considered optimization problem. The rationale is that if the relevant statistical information is captured by the method, the result should not vary too much with the data input. Along these lines, in [8] it is shown that primal regularization does not affect the statistical properties of the solution and the number of iterations required by algorithms based on cutting planes. In our tests, solving the regularized model required slightly more iterations.

4.2.1 Primal Simulation

This is the primal policy (26) available only with the rolling-horizon solvers RH and RRH. It is not possible to benchmark the output with SDDP because this (multi-stage) method lacks a primal policy. The comparison with SDDP is done in the next section, when assessing the dual policies.

For this simulation we keep the fist-stage decisions: $(v_j^7, v_j^{14}, \ldots, v_j^{7\times 52})$ that come from optimization part and simulate the cost-to-go function with new scenarios $(\mathcal{I}_j^t)$, $t \in A_w$, in the w-th week. For 200 out-of-sample scenarios, Figure 7 shows the performance of both RH and RRH in terms of distribution of the price signals.

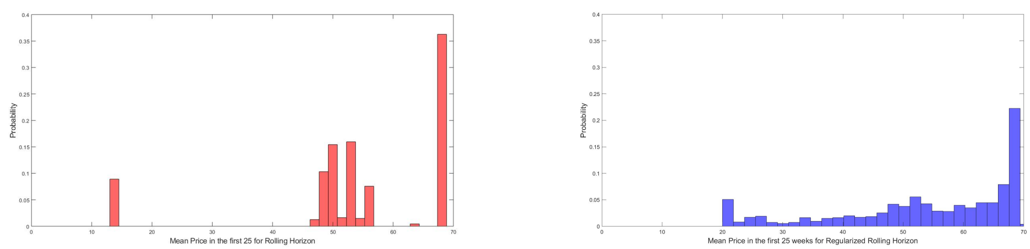

RH   RRH with $\beta = 7000$

Figure 7: Mean price signals of the first 25 weeks, simulated with primal policy of RH and RRH

We observe that the regularized price signal has a smooth distribution, and RRH is less susceptible than RH to variations of different samples. The right graph in Figure 7 is repeated on the left in Figure 8, to contrast the difference in RRH's price distribution when increasing the regularization parameter (on the right, $\beta = 100000$).

In the right histogram in Figure 8 the shift to the left indicates a reduction in the price signals. This is in agreement with the optimization phase: with the primal policy, the higher β, the lower the reservoir levels. Table 1 shows the expected value and variance of the rolling-horizon variants.

	RH	RRH ($\beta = 7000$)	RRH ($\beta = 100000$)
Mean Value	61.22	54.93	13.8
Standard Deviation	16.2	14.31	11.34

Table 1: Price signal mean and deviation for one primal simulation

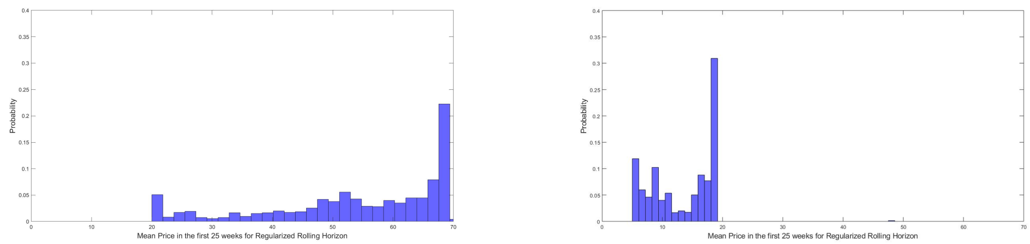

RRH with $\beta = 7000$ RRH with $\beta = 100000$

Figure 8: Mean price signals, simulated with RRH primal policy with two different values for β

In order to evaluate the variability of the approaches under 15 different samples, in Table 2 we measure the variation of the distributions using the Wasserstein distance. The figures in Table 2 show a clear drop in the standard deviation for RRH, reflected also in the Wasserstein distance.

	RH	RRH ($\beta = 7000$)
Mean (Samples)	61.28	53.95
Standard Deviation (Samples)	16.38	14.40
Wasserstein Distance	28.16	15.78

Table 2: Price signal mean and deviation over different primal policies, first 25 weeks

Our final Figure 9, with the level of the reservoirs in the balancing zone NO2 (Norway) shows a typical behavior, observed for all the hydro-plants, with RH exhibiting a more erratic management of the water and keeping lower levels, when compared to RRH. The reason why we see apparently just one blue line is that all paths have close first-stage decisions.

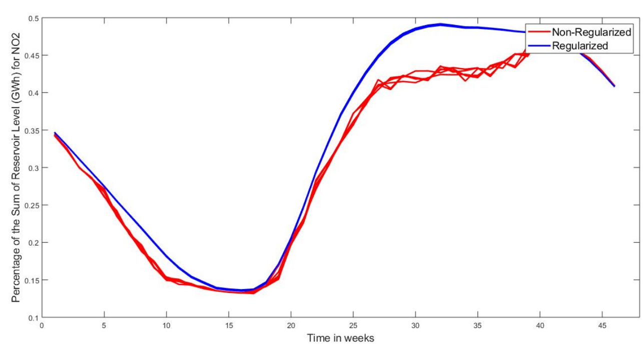

Figure 9: Water management of NO2 with primal simulation

4.2.2 Dual Simulation

The dual policies (27) provided by RH and RRH, are compared with the cuts for the future-cost functions obtained at the optimization phase with SDDP. Using the same set of scenarios employed in the primal simulation reported in Figure 7, we obtain the output in Figure 10. We note that prices vary between 0 and 100 for all approaches, with both SDDP and RH concentrating prices mostly in extreme values and RRH having a better price distribution.

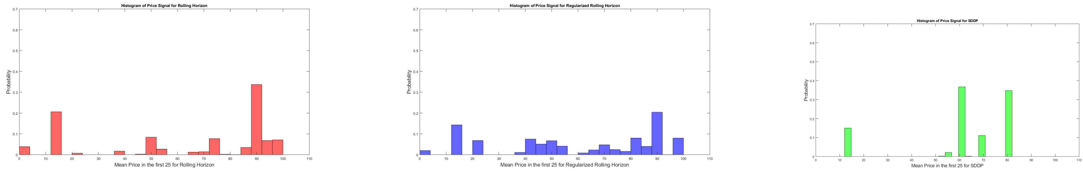

RH RRH SDDP

Figure 10: Mean price signals of the first 25 weeks with dual simulation

The variability of the approaches under different samples, is reported in Table 3. Like with the primal policy in Table 2, we observe once again, though this time with less expressive results, more stability for RRH. Contrary to SDDP, the regularization approach RRH was able to reduce the distance between histograms while keeping the expected value close to the one with RH.

	SDDP	RH	RRH ($\beta = 7000$)
Mean (Samples)	68.2	57.93	58.08
Standard Deviation (Samples)	34.5	38.48	30.1
Wasserstein Distance	6.11	5.64	4.46

Table 3: Price signal mean and deviation over different dual policies, first 25 weeks

We finish our analysis comparing in Figure 11 different paths of the first-stage primal decision that is, the level of reservoirs. Each path consists of a different sequence of scenarios. Each line represents a path and each color a different algorithm.

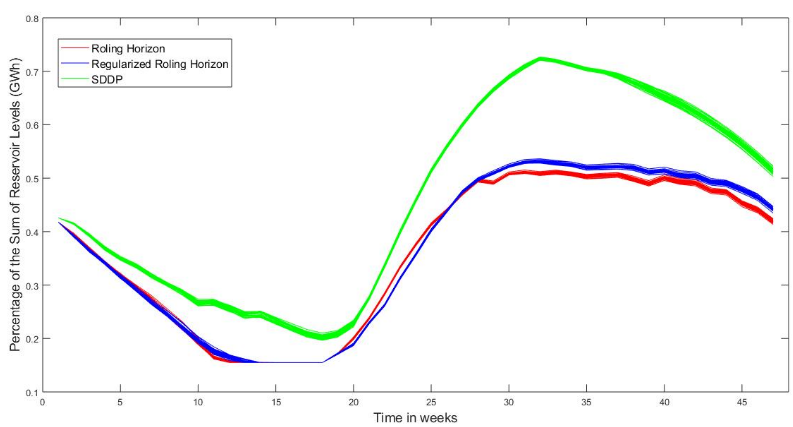

Figure 11: Reservoir dynamics

We observe a similar behavior as with the primal simulation for RH and RRH. For some paths, the curve of the reservoir level in SDDP is distant from the mean curve, as with SDDP prices vary the most. This is a consequence of the prudence of SDDP that, when confronted to a sequence of more favorable scenarios, is forced to a change, with respect to the initial conservative perspective. In terms of quality of the output under simulation, our RRH approach seems to be more stable for the considered sets of runs.

To conclude, we note that the best choice for the penalization/regularization parameter is clearly problem dependent. In our runs, setting its value to $\beta = 7000$ was driven by the constraint violation percentage, inferior to 1%, for the water balance equation.

Concluding Remarks

In many applications dual variables are an important output of the solving process, due to their role as price signals. When dual solutions are not unique, different solvers or different computers, even different runs in the same computer if the problem is stochastic, end up with different price indicators. Even though all of such values are correct, the fact that the obtained dual variable can vary among many possibilities makes unreliable any economic analysis based on marginal prices. We have presented an approach that yields reliable indicators, by providing the minimal-norm multiplier. Our computational experience, both proof-of-concept and on a real-life problem of ENGIE, shows the benefits of the methodology for two-stage stochastic linear programs.

The best choice for the penalization/regularization parameter β is clearly problem dependent. In [12] we propose a performance index similar to the solution concept called *compromise decision* in [19], but adopting a dual point-of-view, to measure bias and variance in multiple replications of sampling-based approximations of two-stage stochastic programs. We observe empirically that our approach yields a significant reduction in the variance of the dual solutions (optimal Lagrange multipliers).

References

[1] A. Bischi, L. Taccari, E. Martelli, E. Amaldi, G. Manzolini, P. Silva, S. Campanari, and E. Macchi. "A rolling-horizon optimization algorithm for the long term operational scheduling of cogeneration systems". In: *Energy* 184 (2019), pp. 73–90.

[2] A. L. Dontchev and R. T. Rockafellar. *Implicit functions and solution mappings: A view from variational analysis*. Springer, 2014.

[3] J. Dupačová, G. Consigli, and S. W. Wallace. "Scenarios for Multistage Stochastic Programs". In: *Annals of Operations Research* 100.1 (2000), pp. 25–53.

[4] L. F. Escudero, J. L. de la Fuente, C. Garcia, and F. J. Prieto. "Hydropower generation management under uncertainty via scenario analysis and parallel computation". In: *IEEE Transactions on Power Systems* 11.2 (1996), pp. 683–689.

[5] A. Gjelsvik, B. Mo, and A. Haugstad. "Long- and Medium-term Operations Planning and Stochastic Modelling in Hydro-dominated Power Systems Based on Stochastic Dual Dynamic Programming". In: *Handbook of Power Systems I*. Ed. by P. Pardalos, S. Rebennack, M. Pereira, and N. Iliadis. Springer, 2010, pp. 33–55.

[6] V. Guigues and C. Sagastizábal. "The value of rolling-horizon policies for risk-averse hydro-thermal planning". In: *European Journal of Operational Research* 217.1 (2012), pp. 129–140.

[7] G. Hechme-Doukopoulos, S. Brignol-Charousset, J. Malick, and C. Lemaréchal. "The short-term electricity production management problem at EDF". In: *Optima Newsletter - Mathematical Optimization Society* 84 (Oct. 2010), pp. 2–6.

[8] J. L. Higle and S. Sen. "Finite master programs in regularized stochastic decomposition". In: *Mathematical Programming* 67.1 (1994), pp. 143–168.

[9] K. Hoyland and S. Wallace. "Generating scenario trees for multistage decision problems". In: *Management Science* 47 (2001), pp. 295–307.

[10] A. J. King and R. T. Rockafellar. "Sensitivity analysis for nonsmooth generalized equations". In: *Mathematical Programming* 55.1 (1992), pp. 193–212.

[11] B. Kummer. “Generalized equations: Solvability and regularity”. In: *Sensitivity, Stability and Parametric Analysis*. Vol. 21. Mathematical Programming Studies. Springer Berlin Heidelberg, 1984, pp. 199–212.

[12] C. Lage, C. Sagastizábal, and M. Solodov. “Multiplier Stabilization Applied to Two-Stage Stochastic Programs”. In: *Journal of Optimization Theory and Applications* 183.1 (2019), pp. 158–178.

[13] Y. Liu, H. Xu, and G.-H. Lin. “Stability Analysis of Two-Stage Stochastic Mathematical Programs with Complementarity Constraints via NLP Regularization”. In: *SIAM Journal on Optimization* 21 (2011), pp. 669–705.

[14] V. L. de Matos and E. C. Finardi. “A computational study of a stochastic optimization model for long term hydrothermal scheduling”. In: *International Journal of Electrical Power & Energy Systems* 43.1 (2012), pp. 1443–1452.

[15] A. Papavasiliou and S. S. Oren. “Multiarea Stochastic Unit Commitment for High Wind Penetration in a Transmission Constrained Network”. In: *Operations Research* 61.3 (2013), pp. 578–592.

[16] A. Philpott and V. de Matos. “Dynamic sampling algorithms for multi-stage stochastic programs with risk aversion”. In: *European Journal of Operational Research* 218.2 (2012), pp. 470–483.

[17] M. V. F. Pereira and L. M. V. G. Pinto. “Multi-stage stochastic optimization applied to energy planning”. In: *Mathematical Programming* 52.1 (1991), pp. 359–375.

[18] S. Rebennack. “Combining sampling-based and scenario-based nested Benders decomposition methods: application to stochastic dual dynamic programming”. In: *Mathematical Programming* 156.1-2 (2016), pp. 343–389.

[19] S. Sen and Y. Liu. “Mitigating Uncertainty via Compromise Decisions in Two-Stage Stochastic Linear Programming: Variance Reduction”. In: *Operations Research* 64.6 (2016), pp. 1422–1437.

[20] A. Shapiro. “Analysis of stochastic dual dynamic programming method”. In: *European Journal of Operational Research* 209.1 (2011), pp. 63–72.

[21] A. Shapiro, D. Dentcheva, and A. Ruszczyński. *Lectures on Stochastic Programming: Modeling and Theory*. Ed. by M. P. Society. MPS–SIAM Series on Optimization. SIAM - Society for Industrial and Applied Mathematics, 2009, p. 436.

[22] A. Street, A. Brigatto, and D. M. Valladão. “Co-Optimization of Energy and Ancillary Services for Hydrothermal Operation Planning Under a General Security Criterion”. In: *IEEE Transactions on Power Systems* 32.6 (2017), pp. 4914–4923.

[23] C. Villani. “The Wasserstein distances”. In: *Optimal Transport*. Vol. 338. Grundlehren der mathematischen Wissenschaften (A Series of Comprehensive Studies in Mathematics). Springer, 2009, pp. 93–111.

[24] S. W. Wallace and S.-E. Fleten. “Stochastic Programming Models in Energy”. In: *Stochastic Programming*. Vol. 10. Handbooks in Operations Research and Management Science. Elsevier, 2003, pp. 637–677.

[25] S. Zaourar and J. Malick. “Prices stabilization for inexact unit-commitment problems”. In: *Mathematical Methods of Operations Research* 78.3 (Dec. 2013), pp. 341–359.